



NANOCELLULOSE-COATED CARBON FIBERS TOWARDS DEVELOPING HIERARCHICAL POLYMER MATRIX COMPOSITES

Braian E.B. Uribe, Alessandra C. Soares-Pozzi, José R. Tarpani*

Sao Carlos School of Engineering (EESC-USP), 13.566-590, Sao Carlos-SP, Brazil

*Corresponding author: jrpan@sc.usp.br

<https://doi.org/10.21452/bccm4.2018.13.09>

Abstract: 0.1, 0.25 and 0.5 wt% microfibrillated cellulose (MFC) aqueous suspensions were used to impregnate carbon fiber fabric via aspersion and immersion to build cost-effective hierarchical polymer matrix composite laminates with enhanced load carrying capacity. Mechanical performance improvements of 28 and 21% were obtained in terms of ultimate tensile strength for 0.1 wt% MFC suspension via aspersion and immersion routes, respectively. The same impregnation conditions provided increments in tensile toughness of 52 and 31%, respectively, showing the positive role of the nanostructure as a strong interfacial agent. MFC solution aspersion was determined as the best impregnation procedure towards strengthening and toughening of the final product.

Keywords: Carbon fibers; Microfibrillated cellulose; Interphase, Mechanical properties.

1. INTRODUCTION

In recent years there has been strong interest in developing polymer matrix composites presenting at least one of their main phases on the nanometric scale [1]; Such materials offer advantages compared to micro- and macro-scale composites that depend not only on the properties of each individual constituent, but also on their morphological and interfacial characteristics [2]. The use of aqueous suspensions to coat continuous fibers with cellulose-based nanofillers has been shown to be an accessible alternative method to improve the mechanical performance of cost-effective polymer composites [3,4]. In the present work an attempt is made to coat carbon fibers with MFC using two different impregnation methods, namely aspersion and immersion, followed by resin infusion under flexible tooling (RIFT) as the manufacturing technique [5,6]. Additionally, an unexplored route based on the use of phosphotungstic acid (PTA) for the selective positive staining of hydroxyl groups [7] was carried out to contrast the nanocellulose interphase via backscattering electron microscopy. This work thus presents information of interest to both academic research and industrial application of polymer composites, with its focus in the field of hierarchical structures.

2. MATERIALS AND METHODS

MFC was synthesized from eucalyptus and was provided by Suzano Pulp and Paper™, Brazil, in the form of water suspension. Continuous PAN-based unsized carbon fiber in the form of 0.30 mm-thick bidirectional plain-weave fabric with areal weight of 200 g/m², 5 bundles/cm in both the warp and weft directions, and 3K filaments per bundle, as provided by Fibertex Brazil™, was employed as the main reinforcing structure. A liquid system composed of Araldite LY 5052 epoxy resin and Aradur 5052 hardener purchased from Huntsman™ Brazil was selected as the polymer matrix.

2.1 COMPOSITE PREPARATION

2.1.1 MFC impregnation of carbon fiber fabric (CFF)

Unsized CFF dry preforms were coated using immersion and aspersion coating processes. Immersion was carried out by dipping the fabrics in aqueous MFC suspension (0.1, 0.25 and 0.5% MFC by weight) for 60 seconds. The spray process was developed using the above-mentioned MFC concentrations and a Western Spray-Gun™ equipped with a 1.5 mm diameter nozzle. Pressure and application distance were maintained constant at 300 kPa and 250 mm, respectively, to impregnate the fabrics. Coated fabrics were subsequently dried in an oven for 3 h at 102 °C until weight loss stopped.

2.1.2 Manufacture of composite laminates

Five plies with in-plane dimensions of 300 x 300 mm², each comprising an unsized CFF covered with MFC, were piled up according to the quasi-isotropic sequence [(0/90),(45),(0/90),(45),(0/90)]. The resin system was degassed at -93 kPa for 8 minutes at an ambient temperature of 25 °C and vacuum assisted liquid resin infusion was then carried out using the same set of pressure and temperature given above. A period of 10 min was spent infusing each composite plaque, giving rise to 1.5 mm-thick laminates. Initial curing was carried out for 24 h under vacuum bagging pressure of -50 kPa at ambient temperature. Post curing was performed in an electric oven for 1 h at 90 °C. The same conditions were applied to build baseline laminates comprising unsized CFF. To differentiate each composite condition, laminates were designated as follows:

CF: Baseline composite laminate (neat CF fibers), I1: 0.1wt.% MFC suspension deposited by immersion, I2: 0.25wt.% MFC suspension deposited by immersion, I5: 0.5wt.% MFC suspension deposited by immersion, A1: 0.1wt.% MFC suspension deposited by aspersion), A2: 0.25wt.% MFC suspension deposited by aspersion, A5: 0.5wt.% MFC suspension deposited by aspersion

2.2 CHARACTERIZATION

2.2.1 Scanning Electron Microscopy (SEM)

Inspection of the topology and morphological features of coated CF surfaces was carried out using a low vacuum, high-resolution FEI Inspect F50™ Field Emission SEM, with the examined surfaces previously sputter-coated with electrically conductive ultra-thin layers of carbon to improve imaging quality. Secondary electron imaging mode was employed at low accelerating voltages ranging from 2 to 10 kV. To assess the interphase, SEM backscattering mode was used at a voltage of 15 kV. Samples were subjected to selective staining of Hydroxyl groups with PTA.

2.2.2 Atomic Force Microscopy (AFM)

Surface assessment of each type of coated CF sample was carried out using an NX-10 Park Systems™ AFM. Silicon probes provided by NCHR Nanoworld™ with a resonance frequency of 320 KHz and a spring constant of 42 N/m were employed to scan the respective surfaces. To perform the measurements, CF and MFC as isolated phases, as well as the CFF/MFC arrangements were mounted onto a metallic stub with a flat Mica lamella surface. Whenever necessary, fast-curing Araldite™ adhesive was used to attach each sample to the lamella. Finally, the images were processed in the open platform software Gwyddion™.

2.2.3 Stereoscopy

CF surface was observed before and after coating with MFC using a Zeiss Discovery™ V8 stereoscope at 5x magnification. Image acquisition was carried out using an AxioCam Erc™ 5s integrated camera, and subsequent image analysis in the open platform software ImageJ™.

2.2.4 Transmission electron microscopy (TEM)

TEM studies were performed using FEI Titan Low-Base™ microscope working at 80 kV and equipped with a CESCOR Cs™ probe corrector, an ultra-bright X-FEG™ electron source and a monochromator. TEM imaging was performed with the high-angle annular dark field (HAADF) detector. Composite sections with ~60 nm in thickness were produced via focused ion beam (FIB).

2.2.5 Contact angle measurements

The produced materials were analyzed at room temperature with KSV CAM101™ equipment. Measurements were performed for each composite condition as well as for neat CF and epoxy resin, examining three samples of each type of material and taking three measurements per sample. The method used for the contact angle assessment was based on the measurement of the contact angle of a drop of water deposited onto the surface of treated and untreated fiber bundles.

2.2.6 Mechanical testing

Mechanical testing was performed in an EMIC™ model 23-100 electromechanical universal testing machine equipped with a 10 kN load cell and an axial extensometer with an original gauge length of 25 mm. In tensile mode, five test coupons with in-plane dimensions 250 x 22 mm² were used for each class of composite laminate. Tests were carried out according to the ASTM-D3039-08 standard under displacement-controlled conditions, with the test speed fixed at a speed of 2 mm/min.

3. RESULTS AND DISCUSSION

3.1 Comparison of impregnation routes

The amount of MFC deposited onto CF by immersion and aspersion, respectively, are plotted in Figure 1. The aspersion method was more efficient for nanostructure deposition within the entire range of MFC concentrations studied, attaining the peak at 0.25wt% MFC suspension in water.

Interesting to note that the water dependency of each impregnation method is crucial to optimize the deposition process.

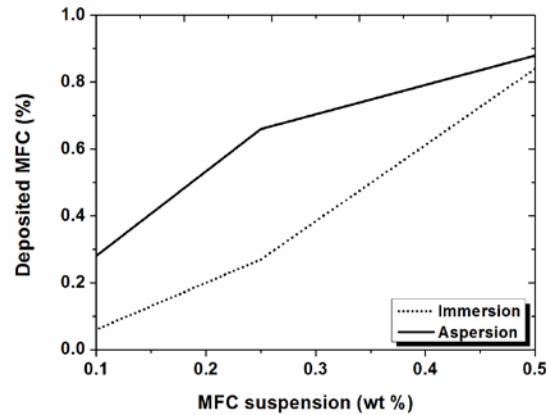


Fig. 1: Amount of deposited MFC onto CF as a function of the MFC concentration for immersion and aspersión impregnation routes.

3.2 Phase morphology

Isolated carbon microfibers and MFC nanofibers, as well as their assembling, were observed via different microscopy techniques at increasing image magnification, as shown in Figure 2.

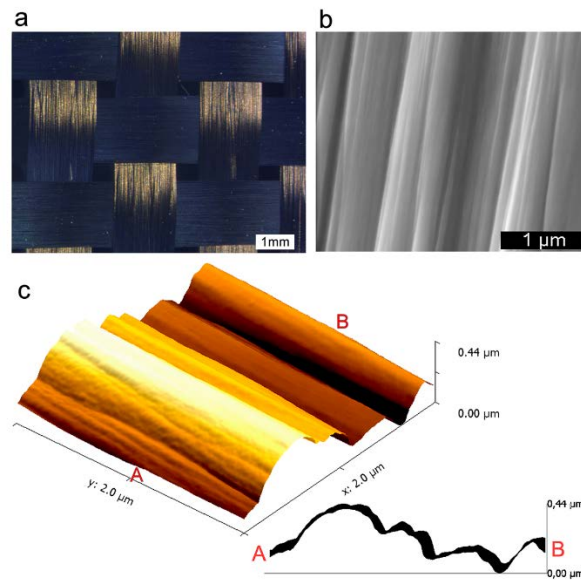


Fig. 2: Three distinct views of CF surface: (a) Stereoscopy, (b) FEG-SEM, and (c) AFM (inset corresponds to the height profile measured along the segment AB).

The irregular surface topography (12 nm roughness) suggests the possibility of mechanical interlocking between the main constituents of the composite.

MFC was also analyzed via AFM as shown in Figure 3, with shape and size features being revealed. The main nanofibres are < 75 nm in height, which are linked to minor substructures of ~30 nm, therefore forming a hierarchical array. This complex nanostructure trends to provide efficient load transfer and distribution along the whole nanophase element, resulting in cooperative dynamics of the thinner nanofibrils acting as an energy dissipater for the thicker ones. The compatibility of carbon micro fiber / MFC nanofiber is based upon mechanical anchoring mechanism [8,9]. However, previous studies have also shown the generation of hydroxyl and

carbonyl groups on the CF surface when exposed to atmospheric oxygen [10], thus suggesting that Van der Waals interactions might cooperate to MFC / CF interaction owing to the reactivity of the OH- groups present on the MFC surface [11].

Roughness of MFC / CF array was determined as 79.5 nm. This substantial increase in surface roughness (700%), when compared to neat CF, gives rise nano- and microcavities, creating multiple points of mechanical anchorage for the solid resin after infusion process, leading to strong and efficient matrix / reinforcement interplay.

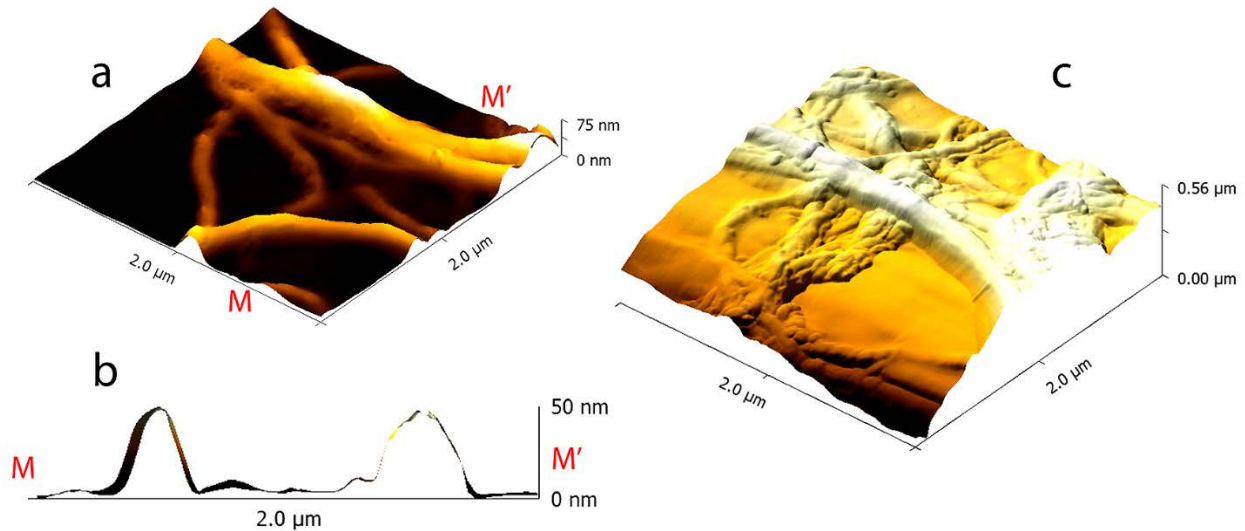


Fig. 3: (a) AFM micrograph of MFC structure; (b) Height profile measured along the segment MM'; (c) MFC deposited onto a CF filament.

3.3 MFC-impregnated CF

Stereoscopic analysis produced the images displayed in Figure 4, where the insets correspond to FEG-SEM secondary electron images of MFC impregnated-CF regions. Immersion process trends to induce nanostructure coalescence with increasing MFC suspension concentration, leading to greater heterogeneity as compared to the aspersion method. By contrast, the latter process trends to generate thinner coatings with evenly MFC distribution and higher solid content.

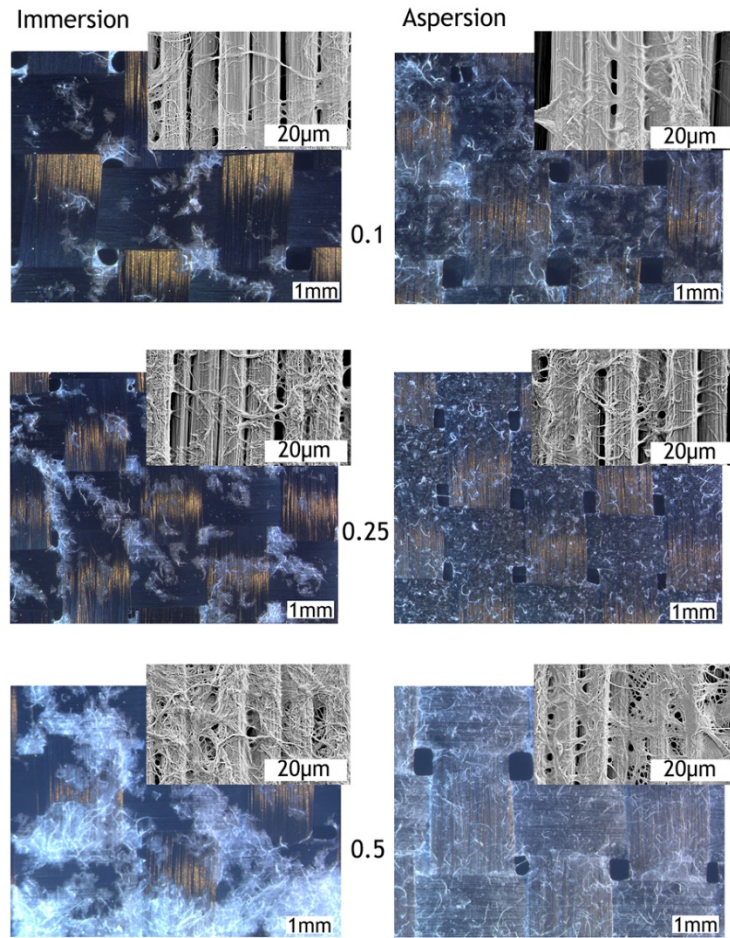


Fig. 4 Stereoscopic and FEG-SEM images of MFC-coated CF via immersion and aspersion routes, respectively. MFC solution concentration are indicated.

3.4 Interphase analysis

HAADF secondary electrons micrographs referring to the minimum interphase thickness of A1 sample are presented in Figure 5.

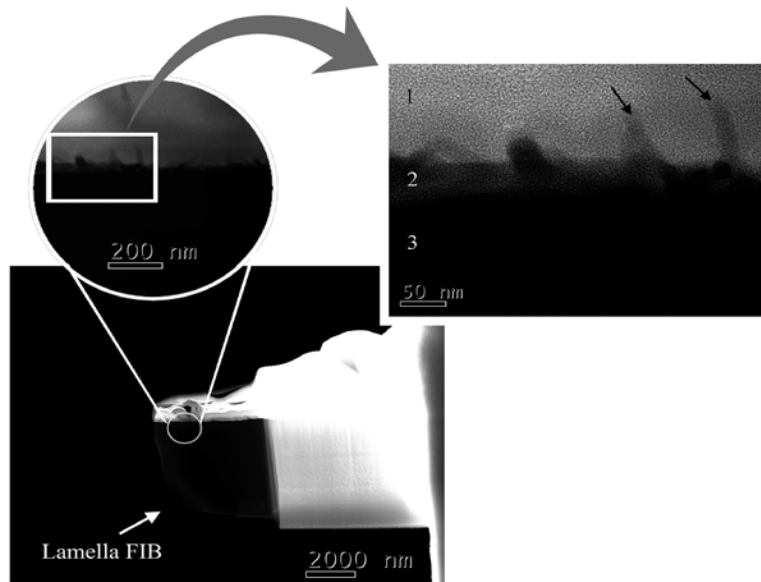


Fig. 5 HAADF STEM micrographs displaying matrix / fibre interphase in composite A1.

MFC coating resulted in an interphase with visible nanofibres (black arrows) and orthogonally aligned towards the main CF. The average widths of the nanofibres and interphase were 20 ± 6 nm and 40 ± 1 nm, respectively. FC / MFC aspect ratio equals 175. Figure 6 displays FEG-SEM micrographs of the composite interphase in arrangement A1, where the inhomogeneous nature of the microfibrillated cellulose, due to its defibrillation during the synthesis process, is seen [12].

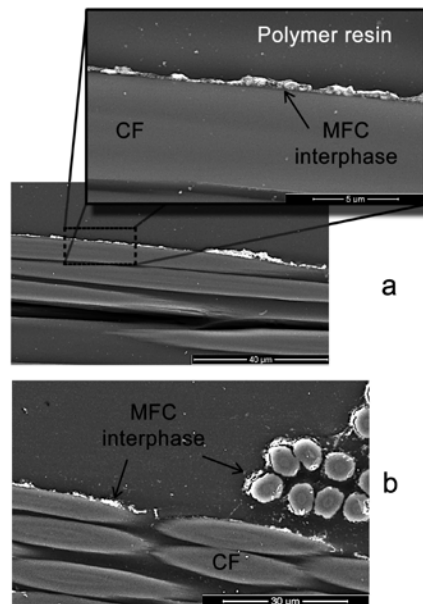


Fig. 6 Composite interphase aspect as seen via BSE-FEG for CF directions: (a) 0°, (b) 45° and 90°. MFC treated with phosphotungstic acid (PTA) as the selective staining agent.

Minimum and maximum interphase widths were calculated at 150 and 2.0 μ m, with an increasing trend to wider interphase for CF oriented from 0° to 90°.

3.5 Contact angle measurement

Figure 7 shows that the epoxy resin matrix presents low water wettability (hydrophobic character). By contrast, unsized CF displays intermediate value, which was further reduced with the deposition of MFC, denoting increasing adhesion potential [13,14]. This indicates that MFC can be recommended for use in composite systems having polar resin matrices.

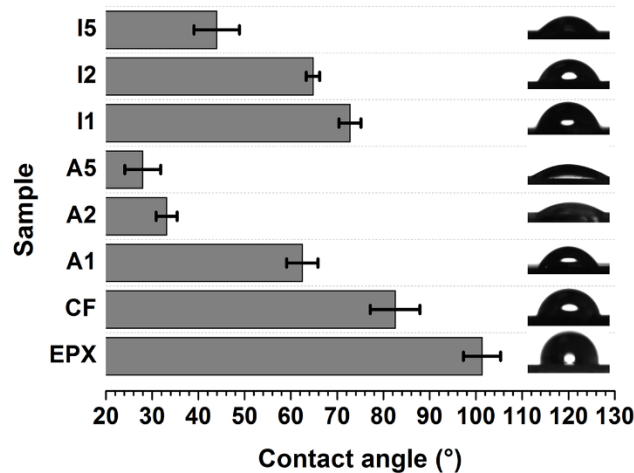


Fig. 7 Contact angle measurements.

As shown in Figure 7, aspersion MFC deposition provides the lowest contact angle, therefore evidencing its high potential for generating wettable CF surfaces for MFC contents lower than 0.28% on a CF weight basis.

3.6 Mechanical properties

Figure 8 shows tensile stress-strain curves for the studied composites. For the aspersion process, the most favorable result was verified in CF impregnated with 0.1wt% aqueous suspension, leading to an increase of 28% in ultimate strength as compared to the baseline condition (neat CF). By contrast, the same impregnation route using MFC concentrations of 0.25 and 0.5wt% impacted negatively that mechanical tensile property.

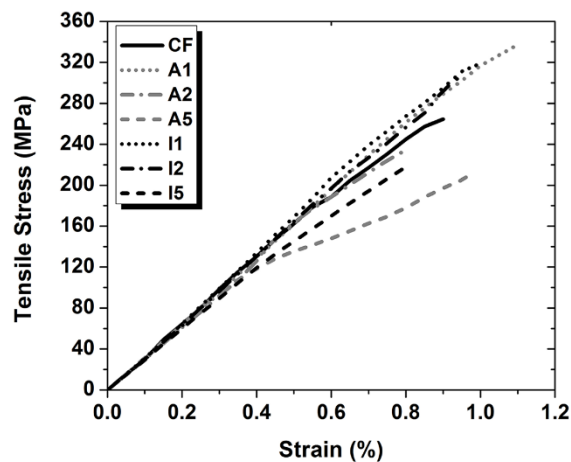


Fig. 8 Stress-strain curves obtained from tensile testing.

For the immersion route, whereas conditions of 0.1 and 0.25wt% MFC suspension resulted in increased tensile strength of 21 and 16%, respectively, the mechanical response of CF coated with 0.5wt% MFC was impaired by 18%. The tensile strength improvement in sample I1 is similar to values reported in the literature [3]. From the results, it can be hypothesized that lower MFC amounts provides more effective hydrogen bonding between hydroxyl groups present in both phases, i.e., optimized water absorption level [15]. Tensile stiffness was practically the same for all composites formulations, indicating that at lower strains the role of MFC in restraining polymer chain movement is negligible. In previous study [3], the authors found MFC improving tensile modulus by 28% for non-post-cured composites. This point needs further study and clarification. Toughness at ultimate load, corresponding to the area underneath the stress-strain curve, was discovered to increase from 31 to 52% for I1 and A1 samples, respectively, permitting one to conclude that aspersion process is substantially more efficient than immersion route in providing toughening via fiber bridging [16].

3.7 Fractographic analysis

Figure 9a presents the composite structure of sample A1 after tensile fracture, which portrays well-adhered and consolidated interlayers (white arrow). Propagation of cracks in the middle zone resulted in catastrophic failure, possibly associated with a high local concentration of nanofibrils. As shown in Figure 9b, nanocellulose-rich region (black arrow) acts as a bridge joining solid blocks of resin to the CF reinforcement. This micrograph also shows the surrounding nanophase regarding the CF surface. Several thicker fibrils can be observed in Figure 9c, indicating the saturation of the CF surface with MFC, which decreased the adhesion of the main composite constituents due the remarkable difference in surface energy between the resin and the treated CF surface (see Figure 7 referring to A5 sample). microfracture displayed in Figure 9d reveals a catastrophic interphase rupture, indication that deposited MFC can act as a stress concentration region as well. By contrast, Figure 10 portrays a web-like MFC structure firmly attached to the main composite constituents, indicating the vital role of appropriate control of MFC's branch size and spatial distribution, beside naturally the deposited amount onto CF.

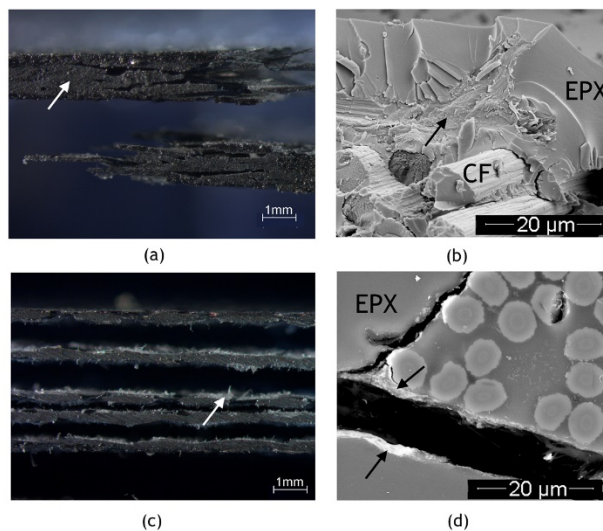


Fig. 9 Fracture surfaces after tensile testing displaying: (a,b) Micro-failure in best-performing sample A1; (c,d) Macro- and micro-failure in worst-performing sample A5.

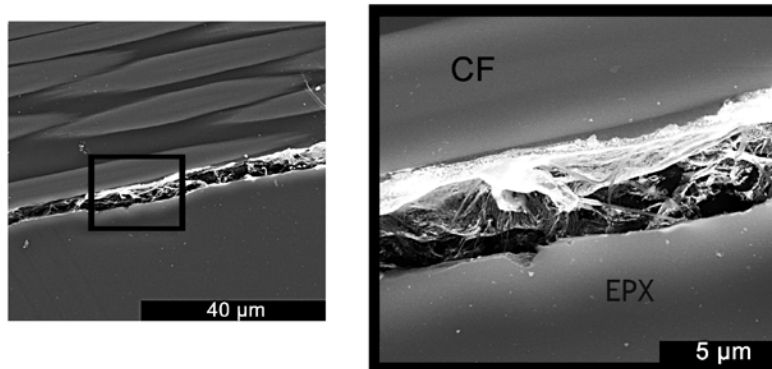


Fig. 10 Composite interphase after tensile fracture.

4. CONCLUSIONS

In this paper, maximum improvement on tensile strength and fracture toughness of hierarchical composite laminates were reached for an MFC concentration in water of 0.1% (0.28% MFC in terms of CF weight), with the aspersion method shown as the more promising MFC / CF impregnation method. Nanocellulose interphase evaluation via electron microscopy techniques was enhanced by selective PTA staining, which provided high contrast for observation in backscattering electron mode.

Acknowledgements: To CNPq-Brazil (Process 140339/2015-9), Dr. Antonio Carvalho and M.Sc. Emanoele Chiromito (SMM-EESC-USP São Carlos, Brazil), Dr. Raul Arenal (Instituto de Nanociencia de Aragon, Universidad de Zaragoza, Spain) and Suzano Pulp and Paper™, Brazil.

5. REFERENCES

- [1] Hussain F. Polymer-matrix nanocomposites, processing, manufacturing, and application: An Overview. *J. Compos. Mater.* 2006, 40, 1511–1575.
- [2] Zhang Q, Liu J, Sager R, Dai L, Baur J. Hierarchical composites of carbon nanotubes on carbon fiber: Influence of growth condition on fiber tensile properties. *Compos. Sci. Technol.* 2009, 69, 594–601.
- [3] Uribe BEB, Chiromito EMS, Carvalho AJF, Tarpani JR. Low-cost, environmentally friendly route for producing CFRP laminates with microfibrillated cellulose interphase. *Express. Polym. Lett.* 2017, 11, 47–59.
- [4] Asadi A, Miller M, Moon RJ, Kalaitzidou K. Improving the interfacial and mechanical properties of short glass fiber/epoxy composites by coating the glass fibers with cellulose nanocrystals. *Express. Polym. Lett.* 2016, 10, 587–597.
- [5] Williams C, Summerscales J, Grove S. Resin infusion under flexible tooling (RIFT): a review. *Compos. Part A Appl. Sci. Manuf.* 1996, 27, 517–524.
- [6] Summerscales J, Searle TJ. Low-pressure (vacuum infusion) techniques for moulding large composite structures. *J. Mater. Des. Appl.* 2005, 219, 45–58.
- [7] Sawyer, L, Grubb, D, Meyers, GF, Eds., *Polymer Microscopy*, 3rd ed., Springer-Verlag: New York, 2008.
- [8] Shi Y, Wang B. Mechanical properties of carbon fiber/cellulose composite papers modified by hot-melting fibers. *Prog. Nat. Sci. Mater. Int.* 2014, 24, 56–60.
- [9] Song W, Gu A, Liang G, Yuan L. Effect of the surface roughness on interfacial properties of carbon fibers reinforced epoxy resin composites. *Appl. Surf. Sci.* 2011, 257, 4069–4074.

- [10] Yip PW, Lin SS. Effect of surface oxygen on adhesion of carbon fiber reinforced composites. *MRS Proc.* 1989, 170.
- [11] Romanzini D, Ornaghi-Junior HL, Amico SC, Zattera AJ. Preparation and characterization of ramie-glass fiber reinforced polymer matrix hybrid composites. *Mater. Res.* 2012, 15, 415–420.
- [12] Chinga-Carrasco G. Cellulose fibres, nanofibrils and microfibrils: The morphological sequence of MFC components from a plant physiology and fibre technology point of view. *Nanoscale Res. Lett.* 2011, 6, 417.
- [13] Ma L, Meng L, Wang Y, Wu G, Fan D, Yu J, et al. Interfacial properties and impact toughness of dendritic hexamethylenetetramine functionalized carbon fiber with varying chain lengths. *RSC Adv.* 2014, 4, 39156–39166.
- [14] Ma L, Meng L, Wu G, Wang Y, Zhao M, Zhang C, et al. Improving the interfacial properties of carbon fiber-reinforced epoxy composites by grafting of branched polyethyleneimine on carbon fiber surface in supercritical methanol. *Compos. Sci. Technol.* 2015, 114, 64–71.
- [15] Chen J, Nakamura T, Aoki K, Aoki Y, Utsunomiya T. Curing of epoxy resin contaminated with water. *J. Appl. Polym. Sci.* 2001, 79, 214–220.
- [16] Philippidis TP, Theocaris PS, Roupakias GS. Delamination prevention in composites by interleaving techniques. *Int. J. Damage. Mech.* 1993, 2, 349–363.